Nano-Structures & Nano-Objects 24 (2020) 100570

Contents lists available at ScienceDirect

Nano-Structures & Nano-Objects

journal homepage: www.elsevier.com/locate/nanoso

Dewetting and interdiffusion mediated evolution of Cu nanolayer/Si(001) interface

Jayanta Kumar Bal [a,*], Satyajit Hazra [b]

[a] Department of Physics, Abhedananda Mahavidyalaya, University of Burdwan, Sainthia, 731234, West Bengal, India
[b] Saha Institute of Nuclear Physics, 1/AF Bidhannagar, Kolkata 700064, India

ARTICLE INFO

Article history:
Received 13 April 2020
Received in revised form 31 July 2020
Accepted 2 September 2020

Keywords:
Surface termination
Passivation
X-ray reflectivity
Dewetting
Interdiffusion
Structure

ABSTRACT

Structural evolution of Cu nanolayer deposited on chemically modified Si substrates has been studied by X-ray reflectivity (XRR), atomic force microscopy (AFM) and scanning electron microscopy (SEM) techniques as a function of time. It is evident from the experimental results that two completely different phenomena, namely dewetting (usually observed for highly abrupt interface system like Ag/Si) and interdiffusion (usually observed for highly diffusive interface system like Au/Si), take place simultaneously or co-exist at the interface of such Cu/Si system and thus can be treated as a model system (showing intermediate of two extreme natures). The dual character of Cu/Si system, however, strongly depends on the chemical species, such as hydrogen and bromine, by which Si surface (dangling bonds) is terminated. For example, the interdiffusion of Cu is found more into the H-terminated Si substrate compared to the Br-terminated one (similar to that of the Au/Si system), while the dewetting is dominant on the Br-terminated Si surface compared to the H-terminated Si (similar to that of the Ag/Si system). Such evolution of growth mainly involves dewetting of Cu on the freshly grown silicon oxide areas on the terminated Si substrate (related to the change in the interfacial energy due to the oxide-growth with time by destroying termination) to change the topography of the Cu nanolayer and also interdiffusion of Cu through the silicon oxide free areas (related to the size and electronegativity differences between Cu and Si) to form a very thin interdiffused layer of Cu into Si.

1. Introduction

Now a days, Cu interconnect technology has replaced Al technology in high performance Si microelectronic devices [1–3], as there is definite gain upon moving from Al (resistivity ≈ 2.7 μΩ-cm) to Cu (resistivity ≈ 1.7 μΩ-cm). Also it is likely that Cu will dominant interconnect technology for Si integrated circuits until some new paradigm is developed [4]. On the other hand, as the metal pitch decreases and the number of metal layers increases, it becomes increasingly important to control the chemical physics and reliability of interconnect structures. It has been observed that the interdiffusion of Cu from the surface into the bulk of the Si chip can adversely affect device performance [5]. In reality, the physics of Cu in Si is more complicated, and is an active area of research. Using first-principles simulations, one group has shown that Cu atom can migrates freely on the H-terminated Si(111) surface and adheres selectively on the oxide-terminated site to grow cluster [6], while the other group suggested that Cu adsorbs strongly to the H-terminated Si surface and that the adsorption energy is significantly dependent on the local bonding environment [7]. Similarly, density-functional theory has been used to predict the stability and diffusion of Cu adatoms near and on the H-terminated Si(001) surface [8], while molecular dynamics simulations has been used to correlate the surface free energy of different crystalline planes as well as the geometrical lattice match rule of the Si surface with the crystalline directionality of the Cu layer at different temperature [9]. It has been suggested that Cu may interact with the dielectric insulator materials to degrade the interface and lead to a loss of adhesion, or Cu may diffusion into the dielectric materials [10,11], which are of particular concern with the Cu technology.

It is known that the native oxide layer, which is usually present on the Si surface, can act as a diffusion barrier at the metal–semiconductor interface [12] and is responsible for the dewetted islandlike growth of metals [12,13]. The removal of oxide layer is possible through surface treatment and termination [12–16]. The nature or the surface free energy of such terminated surface and its stability strongly influence the growth of the metal nanolayers [12,13,17,18]. For example, larger diffusion of Au into Si substrate was observed for H-terminated Si compared to Br-terminated Si [12,17], where atmospheric pressure was also found to play dominant role in such diffusion [18]. On the

* Corresponding author.
E-mail address: jayanta.bal@gmail.com (J.K. Bal).

https://doi.org/10.1016/j.nanoso.2020.100570
2352-507X/

other hand, Ag does not diffuse into Si, rather it makes abrupt interface with the substrate [13]. It has been observed that Ag film is more compact or wetted on the H-terminated Si surface in comparison with Br-terminated one. In case of Cu, which has intermediate tendency to interact with Si substrate [19], the role of native oxide in the interdiffusion of Cu into Si substrate has been studied at elevated temperature [20,21], while the structural and morphological properties of epitaxial Cu/Si(001) system has been carried out at ultra high vacuum conditions [22]. A comparison between Au, Ag and Cu, as optimal metal contact, has been carried out for the metal/alkyl layer/Si junction [23]. However, no attempt has been made to understand the role of Si surface termination on the growth and stability of the Cu nanolayer at ambient conditions using nondestructive techniques, which are of utmost importance.

In this paper we have utilized nondestructive X-ray reflectivity (XRR) technique [24–26], which essentially provides an electron–density profile (EDP), i.e. in-plane (x–y) average electron density (ρ) as a function of depth (z) in high resolution [12,13,27–29], to the understand the initial growth of Cu nanolayers on differently-terminated Si substrates and their time evolution at ambient conditions. Unlike Au/Si and Ag/Si systems [12,13], both interdiffusion and dewetting is observed in the Cu/Si system, which is interesting. The possible reasons for such behavior and its implication are discussed.

2. Material and methods

The n-type Si(001) substrates (of resistivity $\approx$ 5–10 Ω-cm and size about 10×10 mm^2) were terminated differently [12, 13]. First the substrates were sonicated by trichloro-ethylene (10 min) and methyl alcohol (10 min) separately to remove organic contaminations [labeled as O-Si(001)]. Then one set was etched by hydrofluoric acid (HF, 10%) after sonication to remove the native oxide layer and to make them H-terminated [labeled as H-Si(001)], whereas the second set was Br-terminated using 0.05% Br-methanol solution (rinsed thoroughly) after HF etching [labeled as Br-Si(001)]. After drying these substrates were then loaded into a sputtering chamber (T4065, KVS) for Cu deposition, where the power and the argon pressure were maintained at 25 W and 3.2×10^{-3} mbar, respectively. Cu thin films of thickness about 16 nm were deposited using a d.c. magnetron sputtering technique on three Si substrates and were designated as Cu/O-Si(001), Cu/H-Si(001) and Cu/Br-Si(001), respectively.

X-ray reflectivity (XRR): XRR measurements of these films were carried out using a versatile X-ray diffractometer (VXRD) setup [30] as a function of time. VXRD consists of a diffractometer (D8 Discover, Bruker AXS) with Cu source (sealed tube) followed by a Göbel mirror to select and enhance Cu Kα radiation ($\lambda = 1.54$ Å). The diffractometer has a two-circle (θ-2θ) goniometer with quarter-circle Eulerian cradle as sample stage. Scattered beam was detected using a NaI scintillation (point) detector. Data were taken in specular condition, i.e., the incident angle (θ) is equal to the reflected angle (θ) and both are in a scattering plane. Under such conditions, a nonvanishing wave-vector component, q_z, exist which is equal to $(4\pi/\lambda)\sin\theta$. The wave vector has been measured with a resolution of 0.0014 Å^{-1}. Analysis of XRR data has been carried out using Parratt's formalism [31]. For the analysis, each film has been divided into a number of layers including roughness at each interface [12,13]. An instrumental resolution in the form of a Gaussian function and a constant background were also included at the time of data analysis.

Atomic force microscopy (AFM) and scanning electron microscopy (SEM): The topography of the Cu nanolayers on chemically modified Si(001) substrates after equilibrium were mapped through atomic force microscopy (AFM) technique (AutoProbe CP, PSI) at ambient conditions in contact mode using a silicon nitride cantilever (spring constant $\approx$ 0.05 N/m) and pyramidal tip. Scans were performed in constant force mode over several portions of the film. WSXM software [32] has been used for processing and analysis of both AFM images. The topography of the Cu nanolayers on differently terminated Si(001) substrates in larger area and in greater statistics were also mapped through scanning electron microscopy (SEM) technique (Quanta 200, FEG).

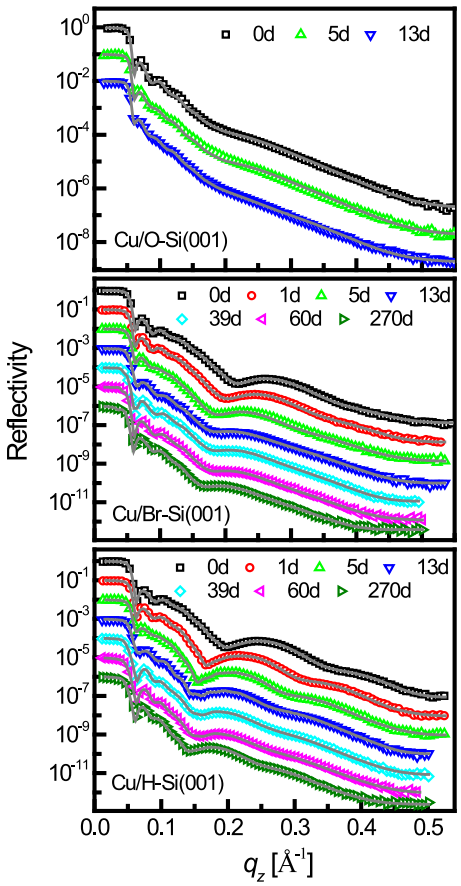

Fig. 1. Time-evolution XRR data (different symbols) and analyzed curves (solid line) of Cu nanolayers on native oxide covered (top panel), Br-terminated (middle panel) and H-terminated (bottom panel) Si(001) surfaces. Data and curves are shifted vertically for clarity. In legends, 'd' indicates the time frame in day scale.

3. Results and discussion

A. *X-ray reflectivity and electron density profile:* Time-evolution XRR data of Cu nanolayers on differently terminated Si(001) substrates at ambient conditions are shown in Fig. 1. Oscillations of smaller and larger periodicities are evident in all curves. The dip corresponding to the larger periodicity shifts toward lower q_z value with time,

which is an indicative of some increment in thickness. The shifts, however, depends on substrate termination. Rapid shift is observed in both H-terminated and Br-terminated Si surfaces (Fig. 1), while negligible shift in native-oxide coated Si surface. The corresponding EDPs obtained from the analysis of the XRR data are shown in Fig. 2. Initially, the fitting was started considering various models. After rigorous trials we found that the five-layer model along with substrate one can achieve major features in all the reflectivity curves. To improve the quality of the fit, individual layer density, thickness and roughness were

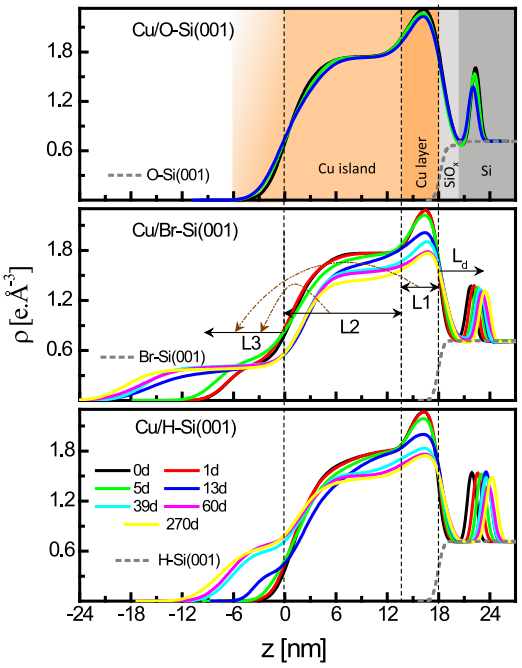

Fig. 2. Analyzed EDPs, which consist of three layers (L1, L2 and L3) above Si substrate and two layers (intermediate layer and Gaussian-shaped layer L_d) into Si substrate as indicated for three samples in three panels. In legends, 'd' indicates the time in day. The constituent layers are presented (top panel) by different colors. The native oxide thickness is found to be 2 nm for oxide sample, but in Br- and H-terminated Si its values are negligibly small.

varied with sufficient iteration ($\approx$ 2000). The Cu thin film located on the Si substrate can be divided in three layers, highly dense L1 layer (layer-like growth) adjacent to the substrate, less dense L2 layer (island-like growth) on top of L1 and the top most L3 layer formed due to dewetting with time. The buried Cu layer L_d consists of two layers, dense Gaussian-shaped layer and an intermediate layer that determines the location of the peak into Si. There are three fitting parameters, such as thickness, density and roughness. Absorption of each layer was kept constant at appropriate values. Notable, the fitting is very sensitive to the thickness, roughness and density of individual layers. However, an error of 1%–2% can be possible in measuring thickness and roughness whereas $\approx$ 10% error can be expected in the estimation of the density of constituent layers. The density of first layer (L1) is the as deposited high density Cu layer (density close to bulk value, 2.27 e.Å^{-3}) of thickness $\approx$ 5 nm attached with the Si substrate; whereas second layer (L2) is the as deposited relatively low density Cu layer of thickness $\approx$ 13 nm above L1 layer and third layer (L3) is very low density Cu layer above L2 layer, the density and thickness of which evolved with time. The buried diffused Cu layer L_d can be divided into two layers: the Gaussian-shaped layer and the intermediate layer. For the Cu/O-Si(001) sample, L3 layer is absent and all the other layers remain unchanged with time; while for the Cu/Br-Si(001) and Cu/H-Si(001) samples, the density and thickness of L3 layer increases in the expense of the density of the L1 and L2 layers; and also the value of L_d increases with time. However, the initial values of different parameters and their variation with time are different for different samples.

In case of Cu/Si system another complicacy is that the reaction between the environmental oxygen with the Cu nanolayer which leads to the CuO_x formation on the top of Cu nanolayer. Oxidation of deposited nanolayer does not happen in case of Au and Ag as they are non-reactive with the oxygen. As the electron density of CuO (1.60 e/Å^3) is less than that of pure Cu (2.27 e/Å^3), the oxidation of Cu may also result in decrement in the electron density which may appear as a decrement of the coverage of Cu nanolayer. The decaying in coverage of Cu nanolayer cannot be correlated with the oxidation of Cu as the former process is very slow (dynamics in 'day' scale) compared to the latter one (dynamics in 'minute' scale). Once the samples are taken out from the magnetron sputtering vacuum chamber (argon pressure $\sim 10^{-3}$ mbar) the Cu nanolayers should readily oxidized. So, the oxidation may cause very small decrement in the electron density of EDP (shown in Fig. 2) in the initial stage of XRR reflectivity measurements but it cannot be responsible for the later stage of decrement in the electron density. Notably, Cu/O-Si(001) does not evolve with time (shown in Fig. 2). It implies that the evolution of Cu/H-Si(001) and Cu/Br-Si(001) occur only due to dewetting and interdiffusion not because of oxidation of Cu otherwise Cu/O-Si(001) would evolve. Moreover, the formation of Gaussian-shaped diffused layer was also observed for Au/Si system [12,13,18]. In normal diffusion one can expect that the concentration decays like error function. In the present study, such peculiar shape is likely to form at the time of Cu deposition through sputtering technique. During sputtering a DC voltage (around 300 V) was applied for eroding the source (here Cu) by plasma. Probably the eroded clusters of source material acquired enough kinetic energy to penetrate into Si substrate during deposition.

B. Topography

Atomic force microscopy: Typical AFM images of Cu nanolayers on O-Si(001), Br-Si(001) and H-Si(001) after prolonged dewetting and interdiffusion are shown in Fig. 3. For the comparison AFM image of Cu nanolayer on O-Si(001) is included in this figure (top panel). The topography, obtained from the AFM images, suggests that all films are composed of islands. Apart from this few scattered big 3D-islands has been observed in Cu/Br-Si(001) and Cu/H-Si(001). In the Cu/Br-Si(001) sample the size of these 3D-islands varies from 180–250 nm whereas in Cu/H-Si(001) sample it varies from 120–150 nm which is smaller relative to the former sample. The shape of the islands in both the samples does not show faceting nature. Moreover, no crystallinity of the Cu nanolayers after prolonged dewetting and interdiffusion has been observed in XRD (not shown here).

Scanning electron microscopy: SEM images of two Cu films, after prolonged evolution due to dewetting and interdiffusion, are shown in Fig. 4. SEM image is taken in order to get an idea about the morphology in large scale. Island like features have been observed in both samples. But few big sized 3D-islands are randomly scattered on the surface as observed in the AFM images. These islands are prominent in Br-terminated sample relative to H-terminated sample.

C. Dewetting and Interdiffusion

Diffusion length L_d, which is measured from the fixed interface position at $z = 180$ Å to the center position of Gaussian-shaped nanolayer, has been calculated from the EDPs and plotted as a function of time in Fig. 5. L_d increases in similar fashion for two samples but the rate of increment is large in Cu/H-Si(001) sample. For Cu/H-Si(001) sample L_d increases from 39 Å to 63 Å whereas for Cu/Br-Si(001) sample L_d increases from 38 Å to 55 Å. It should be mentioned here that L_d for Cu/O-Si(001) sample remains constant nearly around 35 Å. It indicates that the native silicon oxide acts as a barrier for diffusion-font (Gaussian nanolayer) movement into Si, although initial diffused amount (10.7 e/Å^2) is higher compared to Au/Si system (7.1 e/Å^2).

In order to understand the dewetting dynamics of Cu nanolayer we have calculated the dewetted amount of Cu (M_{dewet}) from the L3 layer (shown in EDP) and plotted it as a function of time in

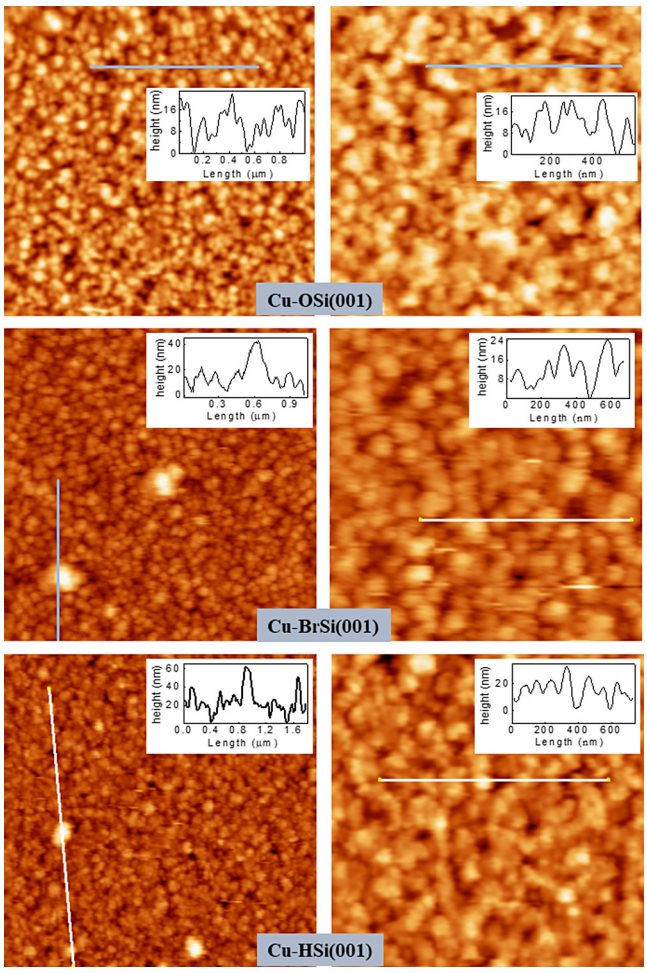

Fig. 3. AFM images of scan size 2000×2000 nm^2 (left) and 1000×1000 nm^2 (right) along with line profiles showing height-variation (in nm) of the three samples.

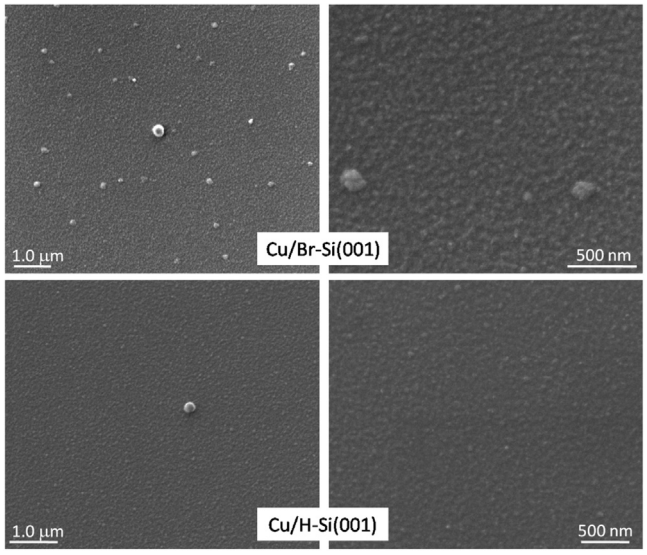

Fig. 4. SEM images of Cu nanolayers on two differently pretreated Si substrates after prolonged dewetting and interdiffusion.

Fig. 6. The amount of dewetting can be quantitatively analyzed using the following general relation:

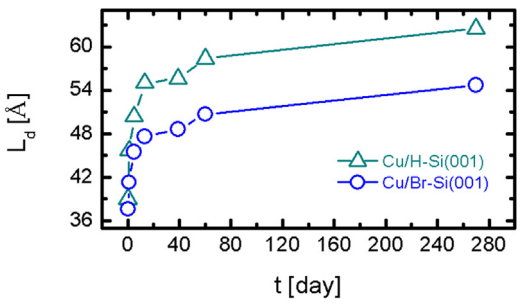

Fig. 5. Diffusion length L_d as a function of time t for two samples.

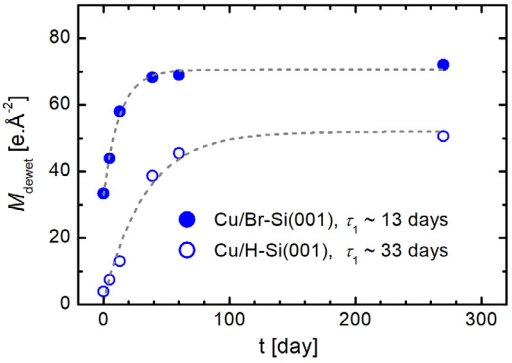

Fig. 6. Dewetted amounts of Cu calculated from L3 layer for two samples as a function of time.

$$M_{dewet}(t) = M_0 + \Delta M[1 - e^{-(t/\tau_3)}],$$

where M_0 is the dewetted amount of Cu obtained just after deposition, $M_0 + \Delta M$ is the maximum dewetted amount reached finally and τ_3 is its growth time. By analysis, the parameters values extracted for two samples are tabulated in Table 1. The M_0 and $M_0 + \Delta M$ values are greater for Cu/Br-Si(001) compared to Cu/H-Si(001) sample which indicates that the dewetting is much more in the former sample from the initial stage. τ_3 value is much greater in Cu/H-Si(001) compared to Cu/Br-Si(001) sample which is the indicative of much rapid dewetting behavior of latter sample.

The coverage of the L1 and L2 layers (C_1 and C_2) and their average (C_a) as calculated from the EDP (of Fig. 2) are plotted in Fig. 7 as a function of time. Corresponding electron density variations are also included in Fig. 7 for comparison. All the coverage decay with time for both the samples due to the dewetting and to some extent interdiffusion of Cu. As the amount of interdiffusion is small (in Cu/H-Si(001) it varies from 13.22 to 19.70 e/Å^2, in Cu/Br-Si(001) it varies from 14.19 to 17.58 e/Å^2) compared to the dewetting of Cu (see Fig. 6), the decrease of C_a takes place mostly due to the dewetting phenomena. At the beginning, there was a big difference in electron density and hence in the coverage between L1 and L2 layers (as evident from both Figs. 2 and 7) though they were formed at the time of deposition. Furthermore, the dewetting dynamics may also be different for these two layers. However, the decay in the coverage for all three cases (L1, L2 and combined layers) follows the same general relation:

$$C_{1/2/a}(t) = C_0 + \Delta C[1 - e^{-(t/\tau_{1/2/a})}]$$

where C_0 is the initial coverage, $C+\Delta C$ is the final coverage; $\tau_{1/2/a}$ is decay time. Analyzed values of these parameters are tabulated

Table 1
Parameters obtained from the analysis of dewetting dynamics for two samples.

Sample	M_0 (e/Å^2)	$M_0 + \Delta M$ (e/Å^2)	τ_3 (day)	C_0 (%)			$C_0 + \Delta C$ (%)			$\tau_{1/2/a}$ (day)		
				L1	L2	Film	L1	L2	Film	L1	L2	Film
Cu/Br-Si(001)	33 ± 1.6	71 ± 1	13 ± 1.4	91	70	75	74	57	62	28 ± 4	14 ± 5	17 ± 5
Cu/H-Si(001)	4 ± 4.2	52 ± 3	33 ± 7	91	65	71	74	60	63	26 ± 4	9 ± 3	13 ± 4

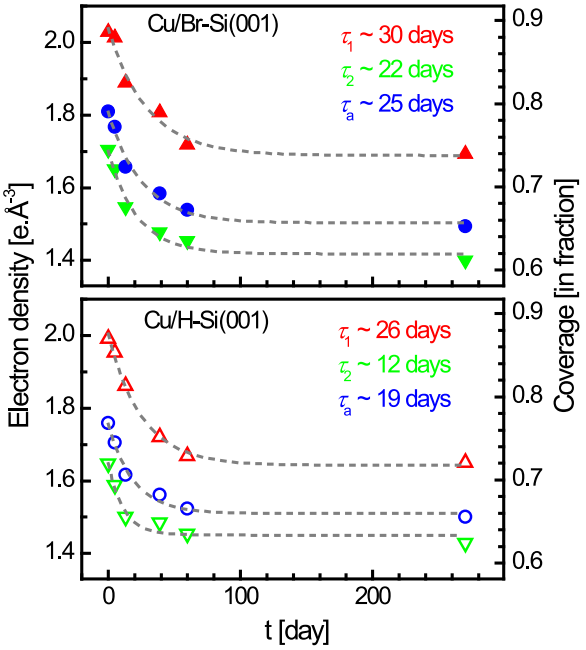

Fig. 7. Variation of electron density and coverage of L1 layer, L2 layer and combined L1+L2 layer with time for two samples in two panels.

in Table 1. C_0 is greater for Cu/Br-Si(001) sample (∼75%) compared to Cu/H-Si(001) (∼71%). It suggests that the overall Cu film is slightly (∼4%) more compact on Br-terminated Si(001) surface in comparison with on H-terminated one. The compactness of lower layer L1 is same for both samples. So, the difference in film coverage is expected to come from the difference in L2 layer coverage. Indeed, there is a ∼5% difference in L2 layer coverage between Cu/Br-Si(001) and Cu/H-Si(001) samples. L1 layer is more compact compared to L2 layer for both samples indicating the layer-plus-island or Stranski–Krastanov (SK) growth of Cu nanolayers on Si surfaces. Final coverages of films and L1 layers for two samples are nearly same although there is a little difference in coverage of L2. The decay time in all three cases (i.e., film. L1 and L2) for two samples are comparable to each other. The decay of Cu nanolayer, just like Ag nanolayer studied previously [9], can be related to the growth of oxide layer at the interface by desorbing the passivating elements like H and Br. From the previous study on Ag/Si we have seen that the τ value is large in case of H-terminated Si surface compared to Br-terminated one whereas in this case τ value is lower for H-terminated surface. This thing can be understood by considering the fact that here since not only the dewetting takes place interdiffusion also takes place. Moreover, the interdiffusion is more in Cu/H-Si(001) sample compared to Cu/Br-Si(001) which may be responsible for slight decaying in coverage as well as lowering in τ value in case of former sample.

To which extent a metal atom diffused into Si depends on multiple factors. The mainly two important factors are the (i) difference between the electronegativity and the (ii) atomic size [33]. If metals (M = Au/Ag/Cu) combine covalently with Si, the binding energy between M and Si is E_{M-Si}, between M, M and Si, Si it is E_{M-M} and E_{Si-Si} respectively. Pauling's empirical relation [34] between electronegativity δ_M, δ_{Si} with those energies can be written as:

$$(\delta_M - \delta_{Si})^2 \infty E_{M-Si} - \sqrt{E_{M-M}E_{Si-Si}}$$

A large difference in electronegativity therefore corresponds to a large difference between the energy of an *M-Si* bond i.e., E_{M-Si}, and the arithmetic mean of the energies of the *M-M* and *Si-Si* bonds. This goes along a stable *M-Si* compound. The second important factor is the atomic size difference between the constituent atoms that has substantial effect on the interdiffusion. In the case of interstitial diffusion of metals into Si single crystals, the difference between the size of metal atoms and the lattice constant of the Si crystal dictates the amount of interdiffusion. It has been seen that constituents with larger size difference exhibits faster interdiffusion and lower activation energy [33].

Table 2
Relevant parameters, such as the resistivity (ρ_R) at room temperature, the electronegativity (δ) in Pauling scale, the covalent atomic radii (R_a).

Element	ρ_R (μΩ cm)	R_a (Å)	δ
Au	2.2	1.44	2.54
Ag	1.6	1.53	1.93
Cu	1.7	1.38	2.00

Previously we have observed only the interdiffusion in Au/Si [12,18] and the dewetting in Ag/Si [13] systems respectively. Here in case of Cu/Si system we observed both phenomena i.e., interdiffusion and dewetting. One part diffuses into Si and another part dewets the Si surface with time. In case of Au and Ag, though both materials are quite similar to each other, i.e., crystal structures, lattice constants and so on, such drastic difference in reactivity has been observed. There is a very slight difference in covalent radius (tabulated in Table 2) which would not be responsible here for different reactivities. Now the only difference which needs to be considered is the electronegativity, i.e., Ag is less negative than Au (given in Table 2) which causes the different reactivity [35]. Braicovich et al. performed a photoemission study [36] of Au/Si system at room temperature and shown that there is a shifting in energy shifts Au(4f) towards lower binding energy and Si(2p) towards higher binding energy. This is due to the electron transfer from Si to Au through the formation of metallic bonding between Si and Au indicating the onset of the room temperature intermixing reaction. It may be quite natural that more electronegative Au is more reactive than Ag. Therefore, the mechanism proposed by Itoh and Gibson [37] is more accurate to state that both the screening effect and the electron transfer must be responsible for the M-Si reaction. Namely, the former triggers the reaction and the latter i.e., electronegativity of the specific metal determines the final reactivity. Since the triggering effect or the breakage of sp^3 tetrahedral coordination in Si by Ag metallic overlayer is clearly shown by Rossi et al. [38], but the low electronegativity of Ag leads to rather weak reactivity. In case of Cu, the intermediate tendency in reaction with Si can be understood considering the combine effect of atomic size and electronegativity of Cu. Although EDP does not provide the information of phase formation at the interface. The covalent radius and electronegativity of Cu (given in Table 2) is slightly

smaller and greater than that of Ag respectively. So these two parameters are mainly responsible for diffusive interface in case of Cu/Si system.

Conclusions

The growth and evolution of Cu/Si system with different passivating elements at the interface have been studied. In all cases co-existence of dewetting and interdiffusion of Cu nanolayer has been observed. Amount of dewetting and interdiffusion strongly depend on surface treatment. Diffusion of Cu into H-terminated Si surface is greater than Br-terminated surface whereas dewetting is dominant on Br-terminated Si surface compared to H-terminated surface. Structure of overlayer films on the three different terminated substrates at the initial stage suggests layer-plus-island (SK) growth which transforms to completely island growth (VW) growth finally. Evolution of growth is through dewetting (related to the change in the interfacial energy due to the oxide-growth), migration and coalesce of Cu, which can even produce 3D-islands on both terminated surfaces and also interdiffusion through native oxide free areas results in a very thin diffused nanolayer of Cu into Si. Small atomic size and medium electronegativity of Cu atoms help to show such mixed behavior with Si surface.

CRediT authorship contribution statement

Jayanta Kumar Bal: Conceptualization, Methodology, Software, Data curation, Writing - original draft, Visualization, Investigation. **Satyajit Hazra:** Supervision, Writing - review & editing.

Declaration of competing interest

The authors declare that they have no known competing financial interests or personal relationships that could have appeared to influence the work reported in this paper.

Acknowledgments

The authors would like to thank S. Chakraborty, and M. Roy for their valuable help in Cu deposition using magnetron sputtering units. J.K.B. thankfully acknowledged to Department of Science and Technology (DST), Government of India, for providing research grant through SERB (CRG/2018/002290) and INSPIRE Faculty Award (IFA13-PH-79).

References

[1] R. Rosenberg, D.C. Edelstein, C.-K. Hu, K.P. Rodbell, Annu. Rev. Mater. Sci. 30 (2000) 229.
[2] S.P. Murarka, S.W. Hymes, Crit. Rev. Solid State Mater. Sci. 20 (1995) 87.
[3] S.P. Murarka, I.V. Verner, R.J. Gutmann, Copper-Fundamental Mechanisms for Microelectronic Applications, Wiley, New York, 2000.
[4] D.R. Lide, CRC Handbook of Chemistry and Physics, CRC Press, New York, 2000.
[5] A.A. Istratov, E.R. Weber, J. Electrochem. Soc. 149 (2002) G21.
[6] K. Tatsumura, T. Watanabe, K. Hara, T. Hoshino, I. Ohdomari, Phys. Rev. B 64 (2001) 115406.
[7] A.S. Foster, M.A. Gosálvez, T. Hynninen, R.M. Nieminen, K. Sato, Phys. Rev. B 76 (2007) 075312.
[8] A. Rodriguez-Prieto, D.R. Bowler, Phys. Rev. B 80 (2009) 155426.
[9] J. Zhang, C. Liu, J. Fan, Appl. Surf. Sci. 276 (2013) 417.
[10] K. Nagao, J.B. Neaton, N.W. Ashcroft, Phys. Rev. B 68 (2003) 125403.
[11] T.-R. Shan, B.D. Devine, S.R. Phillpot, S.B. Sinnott, Phys. Rev. B 83 (2011) 115327.
[12] J.K. Bal, S. Hazra, Phys. Rev. B 75 (2007) 205411.
[13] J.K. Bal, S. Hazra, Phys. Rev. B 79 (2009) 155412.
[14] H.F. Okorn-Schmidt, IBM J. Res. Dev. 43 (1999) 351.
[15] X.G. Zhang, Electrochemistry of Silicon and its Oxide, Kluwer Academic, New York, 2004.
[16] P. Chatterjee, S. Hazra, Soft Matter 9 (2013) 9799.
[17] J.K. Bal, S. Hazra, Defect Diffus. Forum 297–301 (2010) 1133.
[18] J.K. Bal, S. Hazra, Phys. Rev. B 79 (2009) 155405.
[19] A. Cros, P. Muret, Mater. Sci. Rep. 8 (1992) 271.
[20] T. Nakahara, S. Ohkura, F. Shoji, T. Hanawa, Nucl. Instrum. Methods B 45 (1990) 467.
[21] N. Benouattas, A. Mosser, A. Bouabellou, Appl. Surf. Sci. 252 (2006) 7572.
[22] C.A.F. Vaz, S.J. Steinmuller, C. Moutafis, J.A.C. Bland, A.Y. Babkevich, Surf. Sci. 601 (2007) 1377.
[23] M.F. Juarez, F.A. Soria, E.M. Patrito, P. Paredes-Olivera, Phys. Chem. Chem. Phys. 13 (2011) 21411.
[24] I.K. Robinson, D.J. Tweet, Rep. Progr. Phys. 55 (1992) 599.
[25] M. Tolan, X-Ray Scattering from Soft-Matter Thin Films, Springer, Berlin, 1999.
[26] J. Daillant, A. Gibaud (Eds.), X-Ray and Neutron Reflectivity: Principles and Applications, Springer, Paris, 1999.
[27] J.K. Bal, S. Kundu, S. Hazra, Phys. Rev. B 81 (2010) 045404.
[28] I. Roy, S. Hazra, Soft Matter 11 (2015) 3724.
[29] M. Mukhopadhyay, S. Hazra, RSC Adv. 6 (2016) 12326.
[30] S. Hazra, Appl. Surf. Sci. 253 (2006) 2154.
[31] L.G. Parratt, Phys. Rev. 95 (1954) 359.
[32] I. Horcas, R. Fernandez, J.M. Gomez-Rodriguez, J. Colchero, J. Gomez-Herrero, A.M. Baro, Rev. Sci. Instrum. 78 (2007) 013705.
[33] W.-H. Wang, H.Y. Bai, M. Zhang, J.H. Zhao, X.Y. Zhang, W.K. Wang, Phys. Rev. B 59 (1999) 10811.
[34] L. Pauling, The Nature of the Chemical Bond, Cornell University Press, 1962.
[35] A. Hiraki, Surf. Sci. Rep. 3 (1984) 357.
[36] L. Braicovich, C.M. Garner, P.R. Skeath, C.Y. Su, P.W. Chye, I. Lindau, W.E. Spicer, Phys. Rev. B 20 (1979) 5131.
[37] T. Ito, W.M. Gibson, J. Vac. Sci. Technol. A 2 (1984) 561.
[38] G. Rossi, I. Abbati, L. Braicovich, I. Lindau, W.E. Spicer, Solid State Commun. 39 (1981) 195.